Excitation of Ho^{3+} ions via energy transfers from Cr^{3+} and Tm^{3+} ions in (Ca, Zr)-substituted $Gd_3Ga_5O_{18}$ single crystals

1991 J. Phys.: Condens. Matter 3 7887

(http://iopscience.iop.org/0953-8984/3/40/010)

J. Phys.: Condens. Matter 3 (1991) 7887–7894. Printed in the UK

Excitation of Ho^{3+} ions via energy transfers from Cr^{3+} and Tm^{3+} ions in (Ca, Zr)-substituted $Gd_3Ga_5O_{18}$ single crystals

A Brenier, C Madej, C Pedrini and G Boulon

Laboratoire de Physico-Chimie des Matériaux Luminescents (Unité de Recherche associée au CNRS 442), Université Lyon I, 43 boulevard du 11 Novembre 1918, 69622 Villeurbanne, France

Received 4 March 1991

Abstract. (Ca, Zr)-substituted $Gd_3Ga_5O_{12}$ single crystals containing various amounts of Cr^{3+}, Tm^{3+} and Ho^{3+} ions were grown using the Czochralski method. The energy transfers from Cr^{3+} and Tm^{3+} ions were analysed and their quantum efficiencies calculated. The stimulated emission cross section of the $^5I_7$ level of Ho^{3+} in the 1800–2200 nm region was determined using McCumber's theory.

1. Introduction

Eye-safe 2 μm infrared solid state lasers are usually obtained from the $^5I_7 \rightarrow {}^5I_8$ transition of Ho^{3+} impurity in different fluorides, garnets and other oxides. The fluorescence of the Ho^{3+} ions can be sensitized by erbium and thulium impurities in fluorides and by chromium and thulium ions in garnets. In previous papers [1, 2], $Cr^{3+} \rightarrow Tm^{3+}$ and $Tm^{3+} \rightarrow Tm^{3+}$ energy transfers were investigated in detail in (Ca, Zr)-substituted $Gd_3Ga_5O_{12}$ crystals. The results of this analysis are used in the present study of the direct $Tm^{3+} \rightarrow Ho^{3+}$ energy transfer and of the $Cr^{3+} \rightarrow Ho^{3+}$ transfer process via Tm^{3+} ions. The quantum yield of the $^4T_2(Cr^{3+}) \rightarrow {}^5I_7(Ho^{3+})$ transfer and the stimulated emission cross section of the $^5I_7(Ho^{3+})$ level at around 2 μm were deduced. Such information is of particular interest for laser applications.

The experimental techniques used for optical studies and for crystal growth are not described here since they are the same as reported in our previous work [1]. We have grown three crystals by the Czochralski method, containing a nearly constant amount of Cr^{3+} ions and various contents of Tm^{3+} and Ho^{3+} ions (table 1). Chromium ions occupy Ga^{3+} octahedral sites and rare-earth impurities replace Gd^{3+} ions. The segregation coefficient is 2.8 for Cr^{3+} and 1.2 for Tm^{3+} and Ho^{3+}.

2. Excited-state dynamics and energy transfers

The general excited-state dynamics of the triple-doped system is sketched in figure 1, where all the energy levels and the processes considered in the present study are indicated.

0953-8984/91/407887 + 08 $03.50

Table 1. Rare-earth ion concentrations of the samples used for the optical studies, wherein Gd is replaced by $Gd_{1-x-y}Tm_xHo_y$.

x (at.%)	y (at.%)	Cr^{3+} (10^{20} ions cm^{-3})	Tm^{3+} (10^{20} ions cm^{-3})	Ho^{3+} (10^{20} ions cm^{-3})
1	0.5	0.64	1.28	0.60
7	0.5	0.78	9.31	0.53
1	2	0.76	1.22	2.21

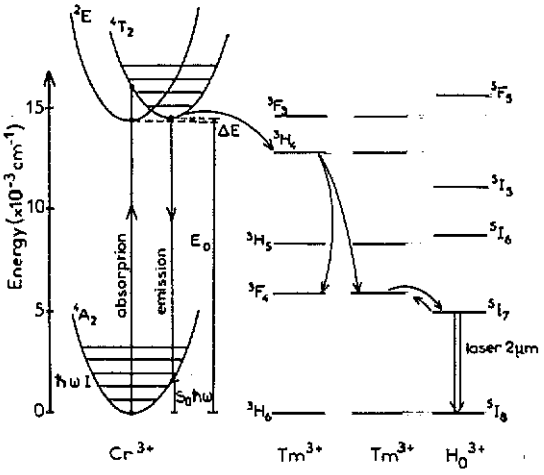

Figure 1. Energy level scheme for the impurity ions and main energy transfer processes.

The addition of 0.5 at.% Ho to samples doped with 1 or 7 at.% Tm does not change the decay of the $^3H_4$ emission significantly. When we add 2 at.% Ho, a weak decrease in the decay time of the $^3H_4 \rightarrow {}^3F_4$ transition is observed, indicating the existence of a weak $^3H_4(Tm^{3+}) \rightarrow Ho^{3+}$ energy transfer. Knowing the microscopic constant P of the $^3H_4(Tm^{3+})$, $^3H_6(Tm^{3+}) \rightarrow {}^3F_4(Tm^{3+})$, $^3F_4(Tm^{3+})$ cross relaxation process, deduced in [1] from the Yokota–Tanimoto [3] equation when the Ho^{3+} ions are absent ($C_{DA} \equiv P = 1.3 \times 10^{-39}\,cm^6\,s^{-1}$), we have calculated the microscopic constant P' of the $^3H_4(Tm^{3+}) \rightarrow Ho^{3+}$ transfer under $^3H_4$ excitation using the same formula:

$$N(t) = N_0 \exp\{-t/\tau - bt^{1/2}[(1 + 10.87x + 15.50x^2)/(1 + 8.743x)]^{3/4}\} \quad (1)$$

in which the contribution of the $Tm^{3+} \rightarrow Ho^{3+}$ transfer was added:

$$b = \tfrac{4}{3}\pi^{3/2}(C_{Tm}\sqrt{P} + C_{Ho}\sqrt{P'}). \quad (2)$$

P' was found to be 70 times weaker than P.

Under Cr^{3+} excitation, a weak $^4T_2(Cr^{3+}) \rightarrow Ho^{3+}$ energy transfer was also observed and, using the previous procedure, its microscopic constant was calculated to be 14 times less than that ($7.7 \times 10^{-39}\,cm^6\,s^{-1}$) characterizing the $^4T_2(Cr^{3+}) \rightarrow Tm^{3+}$ transfer [1].

Let us now consider the energy transfer occurring from the $^3F_4$ lowest excited state of Tm^{3+} to the $^5I_7$ lowest excited state of Ho^{3+}. This transfer is very efficient and can be studied after either $^3H_5$ or $^3F_4$ excitation of Tm^{3+} ions, since the first excitation is followed

by a very fast (less than 1 μs) $^3H_5 \rightarrow {}^3F_4$ relaxation and leads to an exponential $^3F_4 \rightarrow {}^3H_6$ emission (about 1.8 μm) with no rise time in the (Cr, Tm) co-doped crystals [1]. The introduction of Ho^{3+} ions is responsible for the non-exponential faster decay of this fluorescence and simultaneously gives rise to a strong 2 μm $^5I_7 \rightarrow {}^5I_8$ emission transition of the Ho^{3+} ions. In order to describe the $^3F_4(Tm^{3+}) \rightarrow {}^5I_7(Ho^{3+})$ transfer, it is very convenient to follow Chandrasekhar's [4] procedure described in the appendix of [1] when applied to the case of energy transfers.

The application of Markov's method to this problem leads, in the case of dipole–dipole interaction, to a simple expression for the stationary distribution $\omega(\varphi)$ of the transfer rate of a given donor ion D to have a prescribed value φ:

$$\omega(\varphi) = (b/2\pi^{1/2})\varphi^{-3/2} \exp(-b^2/4\varphi) \tag{3}$$

with

$$b = \tfrac{4}{3}\pi^{3/2} C_A \sqrt{P} \tag{4}$$

and

$$\varphi = \sum^{N_A} T_{DA_i}(r_i). \tag{5}$$

C_A is the concentration of acceptor ions A_i, $P \equiv C_{DA}$ is the microscopic constant of the $D \rightarrow A$ transfer, N_A is the total number of acceptor ions, r_i is the distance between D and A_i ions and T_{DA_i} represents the transfer rate on each acceptor A_i.

To describe the transfers, it is therefore correct to use the rate equations for a class φ of ions and their complete resolution is possible, knowing $\omega(\varphi)$. In simple cases, the resolution leads to the well known Inokuti–Hirayama [5] equation. However, the method is of most interest in more complicated cases where the Inokuti–Hirayama formula is no longer valuable.

Returning to the particular case of the $^3F_4(Tm^{3+}) \rightarrow {}^5I_7(Ho^{3+})$ energy transfer, the population $N_\varphi(t)$ of Tm^{3+} ions belonging to the class φ and in the $^3F_4$ excited state decays according to the rate equation

$$\dot{N}_\varphi(t) = -N_\varphi(t)(1/\tau + \varphi) \tag{6}$$

where τ represents the lifetime of $^3F_4$ without any Ho^{3+} ions. The solution of (6) is obvious:

$$N_\varphi(t) = N_\varphi^0 \exp[-t(1/\tau + \varphi)] \tag{7}$$

with

$$N_\varphi^0 = N^0 \omega(\varphi) \qquad \text{at } t = 0. \tag{8}$$

N^0 is the overall initial population of the $^3F_4$ level. The total population $N(t)$ of the $^3F_4$ level is then

$$N(t) = \int_0^\infty N_\varphi(t)\, d\varphi \tag{9}$$

and, taking into account (3), we find that

$$N(t) = N^0 \exp(-t/\tau - b\sqrt{t}) \tag{10}$$

with

$$b = \tfrac{4}{3}\pi^{3/2} C_{Ho} \sqrt{P''}. \tag{11}$$

C_{Ho} is the concentration of Ho^{3+} in the ground state and P'' is the microscopic constant of the $^3F_4 \rightarrow {}^5I_7$ transfer.

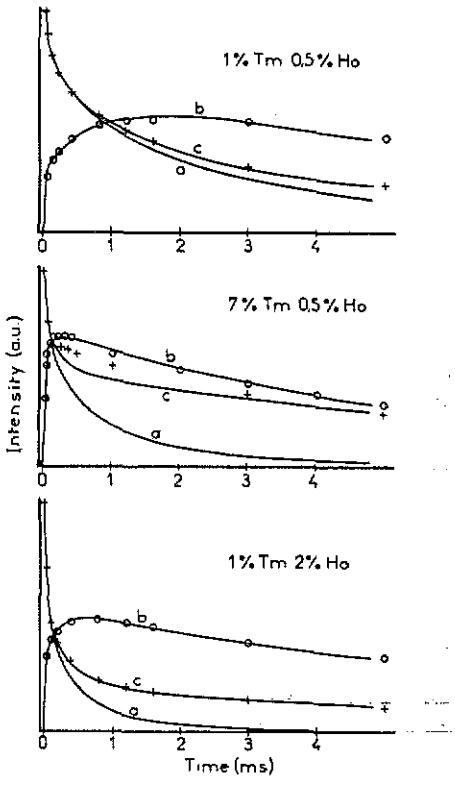

Figure 2. Experimental decays: +, $^3F_4 \rightarrow {}^3H_6$ fluorescence of Tm^{3+}; ○, $^5I_7 \rightarrow {}^5I_8$ fluorescence of Ho^{3+}; ———, best fits to experimental data obtained with the models described in the text.

As previously predicted, in this simple case, equation (10) is simply the Hinokuti–Hirayama formula. It fits the beginning of the experimental $^3F_4 \rightarrow {}^3H_6$ fluorescence (first 100 μs in figure 2 curves a) quite well. However, the rest of the decay is not correctly described. In fact, in $YLiF_4$ and in indium-based fluoride glasses, we had clearly identified an efficient $^5I_7(Ho^{3+}) \rightarrow {}^3F_4(Tm^{3+})$ back transfer [6, 7]. The final parts of the decay of both the $^3F_4$ and the $^5I_7$ levels are similar (figure 2), indicating that such a mechanism actually occurs in the samples at present studied and it has to be included in equation (10). The back transfer is proportional to the number $\omega(\varphi)$ of Tm^{3+} ions of the class φ and to the total number $N'(t)$ of Ho^{3+} ions in the $^5I_7$ excited state, so that equation (6) is replaced by

$$\dot{N}_\varphi(t) = -N_\varphi(t)(1/\tau + \varphi) + k\omega(\varphi)N'(t) \tag{12}$$

where k is the φ-independent back-transfer constant. $N'(t)$ is given by a rate equation analogous to (12) and it turns out that two coupled equations have to be solved. In order to avoid the difficult resolution of such a system, it is better to proceed in the following way. A preliminary fit of $N'(t)$ to the experimental data is first obtained with the expression

$$N'(t) \simeq A_1[\exp(-t/\tau') - \exp(-t/\tau_1)] + A_2[\exp(-t/\tau') - \exp(-t/\tau_2)]. \tag{13}$$

τ' (=9.4 ms) is the lifetime of $^5I_7$ measured after direct excitation of Ho^{3+}; A_i and τ_i are

Table 2. $^3F_4(Tm^{3+}) \rightarrow {}^5I_7(Ho^{3+})$ transfer parameters.

Crystal	P'' (10^{-39} cm^6 s^{-1})	τ (10^{-3} s)	η_T (%)
1 at.% Tm; 0.5 at.% Ho	3.0	11.25	52
7 at.% Tm; 0.5 at.% Ho	14.3	6.0	35.5
1 at.% Tm; 2 at.% Ho	2.1	11.25	—

adjustable parameters without real physical meaning. The best fits lead to curves b in figure 2. The solution of equation (12) is then

$$N_\varphi(t) = N^0\omega(\varphi)\exp\left(-\frac{t}{\tau}-t\varphi\right) + k\omega(\varphi)\left\{\frac{A_1+A_2}{1/\tau+\varphi-1/\tau'}\right.$$
$$\times\left[\exp\left(-\frac{t}{\tau'}\right)-\exp\left(-\frac{t}{\tau-t\varphi}\right)\right]$$
$$\left.-\sum_{i=1}^{2}\frac{A_i}{1/\tau+\varphi-1/\tau_i}\left[\exp\left(-\frac{t}{\tau'}\right)-\exp\left(-\frac{t}{\tau_i}-t\varphi\right)\right]\right\}. \tag{14}$$

The total population $N(t)$ of the $^3F_4$ level is given after integration over φ:

$$N(t) = N^0\exp(-t/\tau - b\sqrt{t} + I \tag{15}$$

where the first term is the Hinokuti–Hirayama expression and I is the result of a numerical integration of the second term of (14) over φ for each value of t.

Equation (15) leads to curves c in figure 2. The best fits were obtained for values of P'' indicated in table 2 (P'' is the microscopic constant of the $^3F_4(Tm) \rightarrow {}^5I_7(Ho)$ transfer). Note that P'' is the only free physical parameter of the model because the intrinsic lifetime τ of $^3F_4$ was separately measured in samples free of Ho^{3+} ions [1]. It should be remarked that, for samples containing 1 at.% Tm, the best fits were obtained with comparable values of P'' and describe the experimental results well. On the other hand, in the case of the heavily Tm-doped sample (7 at.%), the best fit is less satisfactory and was obtained with a much higher value of P''. This is probably because our model does not take into account the energy diffusion between the Tm^{3+} ions which is certainly effective in the case of high concentrated compounds.

Table 2 also gives the quantum yield η_T of the $F_4 \leftrightarrows {}^5I_7$ transfer when the $^5I_7$ population is a maximum. It was deduced experimentally (and not from the theoretical model) for the two samples containing the same amount of Ho (0.5 at.%) and different Tm concentrations (1 and 7 at.%). It is clear that the back transfer induces a strong decrease (about 30%) in the quantum yield in going from 1 to 7 at.% Tm.

3. Quantum yield of the $^4T_2(Cr^{3+}) \rightarrow {}^5I_7(Ho^{3+})$ transfer

The schematic representation of the absorbed energy conversion in (Ca, Zr)-substituted $Gd_3Ga_5O_{12}$ crystals (figure 1) shows that the $^4T_2(Cr^{3+}) \rightarrow {}^5I_7(Ho^{3+})$ transfer takes place

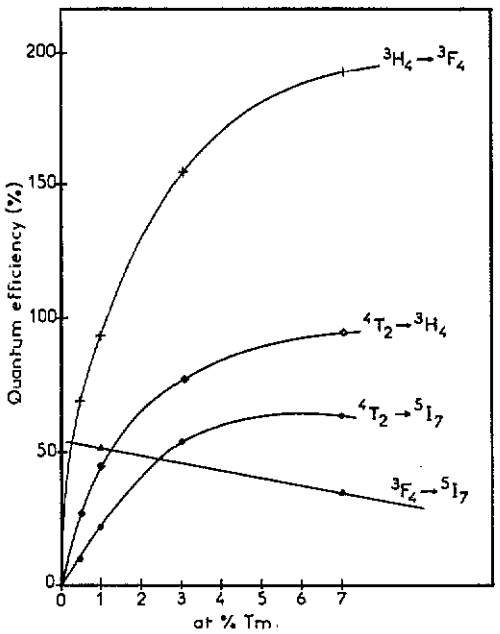

Figure 3. Quantum yields of various transfers in samples containing 0.5 at.% Cr^{3+} and Ho^{3+} and different amounts of Tm^{3+}. The concentrations are nominal.

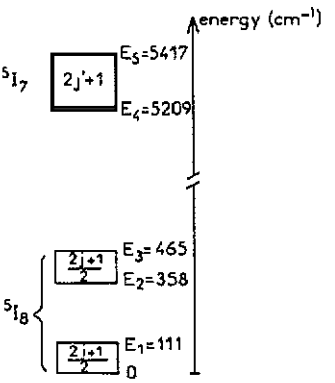

Figure 4. Experimental Stark energy levels of the $^5I_8$ ground state and the $^5I_7$ lowest excited state of Ho^{3+}.

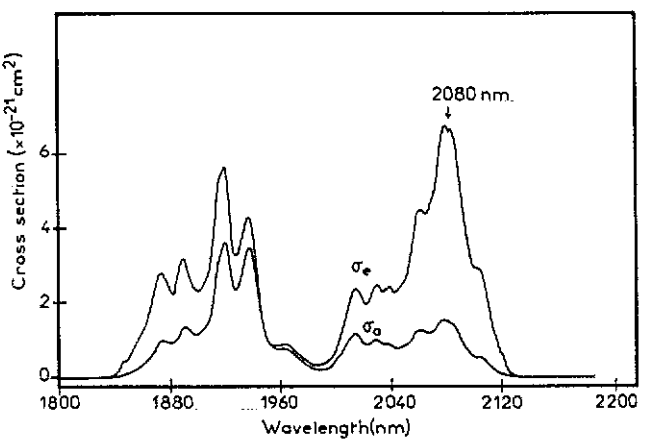

Figure 5. Absorption and stimulated emission cross sections of the $^5I_7(Ho^{3+})$ excited state at room temperature.

in three stages: $^4T_2(Cr^{3+}) \rightarrow {}^3H_4(Tm^{3+})$ energy transfer, $^3H_4(Tm^{3+}) \rightarrow {}^3F_4(Tm^{3+})$ cross-relaxation exchange of excitation between Tm^{3+} ions and $^3F_4(Tm^{3+}) \rightarrow {}^5I_7(Ho^{3+})$ transfer which can be preceded by energy migration between Tm^{3+} ions. The quantum yields of the steps were calculated for samples of constant Cr^{3+} and Ho^{3+} concentrations

(0.5 at.%) and containing different amounts of Tm^{3+} ions. The related curves are displayed in figure 3. The efficiency of the first process $^4T_2 \rightarrow {}^3H_4$ was reported in a previous paper [1]. A good description of the $^3H_4 \rightarrow {}^3F_4$ de-excitation of the Tm^{3+} ions must include the cross relaxation type of energy transfer between the Tm^{3+} ions, the Tm intra-centre de-excitation and the $^3H_4(Tm^{3+}) \rightarrow Ho^{3+}$ direct energy transfer [6]. In order to take into account all these phenomena, the quantum yield of the second $^3H_4 \rightarrow {}^3F_4$ mechanism was evaluated by measuring the relative $^3F_4$ emission intensities obtained after excitations of $^3H_4$ and $^3F_4$, for samples placed inside an integrating sphere. Note that the value of the quantum rate at high Tm concentration is nearly 2 since one Tm^{3+} ion in its $^3H_4$ excited state may lead to two Tm^{3+} ions in the $^3F_4$ state. The efficiency of the third $^3F_4 \rightarrow {}^5I_7$ step was determined in the previous section. Since we have only two experimental points, we have assumed a linear dependence of the quantum yield with Tm concentration. The product of the efficiencies of the three stages finally gives the quantum yield of the $^4T_2(Cr^{3+}) \rightarrow {}^5I_7(Ho^{3+})$ energy transfer. The related curve (figure 3) exhibits a maximum for 5 at.% Tm concentration. This result is important since it shows that, because of the $^5I_7(Ho^{3+}) \rightarrow {}^3F_4(Tm^{3+})$ back transfer, a further increase in Tm^{3+} concentration is not efficient.

4. Stimulated emission cross section of the $^5I_7(Ho^{3+})$ level around 2 μm

The calculation of the gain per unit length of a pumped laser material requires knowledge of the absorption cross section $\sigma_a(\lambda)$ and of the stimulated emission cross-section $\sigma_e(\lambda)$ at the wavelength λ. The latter is given by McCumber's [8] relation

$$\sigma_e(\lambda) = [N^0(^5I_8)/N^0(^5I_7)]\sigma_a(\lambda) \exp[-E(\lambda)/kT]. \tag{16}$$

$E(\lambda)$ is the energy of one photon at the wavelength λ, and $N^0(^5I_8)$ and $N^0(^5I_7)$ are the populations of the $^5I_8$ and $^5I_7$ levels at thermal equilibrium.

The absorption and emission spectra recorded at liquid-helium temperature lead to the energy level scheme of $^5I_8$ and $^5I_7$ Stark levels displayed in figure 4. The ground state can be represented by two thick levels and the excited state by one thick level. The limiting energies E_i of each thick level i are also indicated in the figure. As previously shown [7], the density of the statistical weight g_i of a level i can be evaluated as

$$g_i = d_i/(E_{ih} - E_{il}) \tag{17}$$

where d_i stands for the J degeneracy, and E_{ih} and E_{il} are the highest and lowest energies of the thick level i, respectively: $g = (2J' + 1)/(E_5 - E_4)$ for the $^5I_7$ level; $g = (2J + 1)/2E_1$ for the lowest thick sublevel of $^5I_8$; $g = (2J + 1)/2(E_3 - E_2)$ for the highest thick sublevel of $^5I_8$.

Finally, the Boltzmann law leads to

$$\begin{aligned} N^0(^5I_8) \propto kT\{&[(2J + 1)/2E_1][1 - \exp(-E_1/kT)] \\ &+ [2J + 1/2(E_3 - E_2)][\exp(-E_2/kT) - \exp(-E_3/kT)]\} \\ N^0(^5I_7) \propto kT\{&(2J' + 1)/(E_5 - E_4)[\exp(-E_4/kT) - \exp(-E_5/kT)]\} \end{aligned} \tag{18}$$

with $J = 8$ and $J' = 7$.

Figure 5 shows the curves of $\sigma_a(\lambda)$ and $\sigma_e(\lambda)$ at room temperature. The stimulated emission cross section exhibits a maximum at 2080 nm. Therefore a laser effect from

Ho^{3+} ions in (Ca, Zr)-substituted $Gd_3Ga_5O_{12}$ is expected at around this wavelength. Our simple model of Stark structure of the $^5I_7$ and $^5I_8$ levels predicts a radiative lifetime of $^5I_7$ at around 10.1 ms. This value is close to the experimental decay time of 9.4 ms for the $^5I_7$ level, meaning that non-radiative losses in the $^5I_7 \rightarrow {}^5I_8$ transition are rather low.

5. Concluding remarks

This work shows that efficient energy transfers occur in (Ca, Zr)-substituted $Gd_3Ga_5O_{12}$ garnet from Cr^{3+} to Ho^{3+} impurity ions via Tm^{3+} ions. Optimized systems are obtained with impurity ion concentrations of 0.5 at.% for Cr^{3+} and Ho^{3+} and of 5 at.% for Tm^{3+} owing to the occurrence of $Ho^{3+} \rightarrow Tm^{3+}$ back transfer. Like $Gd_3Sc_2Ga_3O_{12}$ laser material, this garnet could be used to obtain a low threshold 2 μm laser, but at a much lower cost.

Acknowledgment

This research was sponsored by the DGA–Direction des Recherches Etudes et Techniques under grant 88/133.

References

[1] Brenier A, Madej C, Pedrini C and Boulon G 1991 *J. Phys.: Condens. Matter* **3** 203
[2] Brenier A, Madej C, Pedrini C and Boulon G 1991 *J. Lumin.* **48–49** 232
[3] Yokota M and Tanimoto O 1967 *J. Phys. Soc. Japan* **22** 779
[4] Chandrasekhar S 1943 *Rev. Mod. Phys.* **15** 1
[5] Inokuti M and Hirayama F 1965 *J. Chem. Phys.* **43** 1978
[6] Brenier A, Rubin J, Moncorge R and Pedrini C 1989 *J. Physique* **50** 1463
[7] Brenier A, Pedrini C, Moine B, Adam J L and Pledel C 1990 *Phys. Rev.* B **41** 5364
[8] McCumber D E 1964 *Phys. Rev.* **136** 954